Peak and Per-Step Tibial Bone Stress During Walking and Running in Female and Male Recreational Runners

Stacey A. Meardon,*† PT, PhD, Timothy R. Derrick,‡ PhD, John D. Willson,† PT, PhD, Michael Baggaley,§ MS, C. Ryan Steinbaker,‖ MD, Margaret Marshall,† DPT, and Richard W. Willy,¶ PT, PhD
Investigation performed at East Carolina University, Greenville, North Carolina, USA

Background: Athletes, especially female athletes, experience high rates of tibial bone stress injuries (BSIs). Knowledge of tibial loads during walking and running is needed to understand injury mechanisms and design safe running progression programs.

Purpose: To examine tibial loads as a function of gait speed in male and female runners.

Study Design: Controlled laboratory study.

Methods: Kinematic and kinetic data were collected on 40 recreational runners (20 female, 20 male) during 4 instrumented gait speed conditions on a treadmill (walk, preferred run, slow run, fast run). Musculoskeletal modeling, using participant-specific magnetic resonance imaging and motion data, was used to estimate tibial stress. Peak tibial stress and stress-time impulse were analyzed using 2-factor multivariate analyses of variance (speed*sex) and post hoc comparisons ($\alpha = .05$). Bone geometry and tibial forces and moments were examined.

Results: Peak compression was influenced by speed ($P < .001$); increasing speed generally increased tibial compression in both sexes. Women displayed greater increases in peak tension ($P = .001$) and shear ($P < .001$) than men when transitioning from walking to running. Further, women displayed greater peak tibial stress overall ($P < .001$). Compressive and tensile stress-time impulse varied by speed ($P < .001$) and sex ($P = .006$); impulse was lower during running than walking and greater in women. A shear stress-time impulse interaction ($P < .001$) indicated that women displayed greater impulse relative to men when changing from a walk to a run. Compared with men, women displayed smaller tibiae ($P < .001$) and disproportionately lower tibial forces ($P \leq .001$-$.035$).

Conclusion: Peak tibial stress increased with gait speed, with a 2-fold increase in running relative to walking. Women displayed greater tibial stress than men and greater increases in stress when shifting from walking to running. Sex differences appear to be the result of smaller bone geometry in women and tibial forces that were not proportionately lower, given the womens' smaller stature and lower mass relative to men.

Clinical Relevance: These results may inform interventions to regulate running-related training loads and highlight a need to increase bone strength in women. Lower relative bone strength in women may contribute to a sex bias in tibial BSIs, and female runners may benefit from a slower progression when initiating a running program.

Keywords: bone stress injury; biomechanics; gait analysis; female athlete; speed; running

In both men and women, the tibia is one of the most common sites of a bone stress injury (BSI).[56] Women experience a 1.5 and 3 times higher incidence of BSIs in civilian and military populations, respectively.[56] In addition to gait mechanics,[42,43] bone structure, aerobic capacity, muscle size, and diet contribute to the BSI risk.[56] Patients are at a heightened risk for BSIs when workloads are increased, such as when new training regimens are initiated[5] or when run speeds are increased.[16] Return to running programs, consisting of progressive walk-run sessions, are the cornerstone of return to sports for athletes rehabilitating from a BSI.[53] However, the recurrence of BSIs is common,[49] suggesting that bone loads can be better managed during the rehabilitation and postrehabilitation phases. Greater insight into tissue level loads during walking and running may provide better guidance for prescribing workloads in athletes thought to be at risk for BSIs.

Bone stress, which causes bone strain, is a proximate cause of injury that reflects bone strength relative to the imposed load. Activities with highly repetitive bone stresses and strains without adequate rest lead to microdamage accumulation and eventual BSIs.[7] Bone strain,

The American Journal of Sports Medicine
2021;49(8):2227–2237
DOI: 10.1177/03635465211014854

which is thought to be the causal factor for a bone fracture,[37] can be quantified with in vivo strain gauges. Measurements using strain gauges attached to the tibia are invasive and limited to small sample sizes and small regions of bone.[6] Computer-based musculoskeletal models incorporating the bone structure and activity-related forces have been used to estimate bone stress and strain noninvasively. Models range from simplistic, such as modeling the tibia as a hollow ellipse,[30,31,46] to computationally complex using participant-specific bone images with micro–finite element analysis.[18,51] The VA-BATTS tool estimates stress that contributes to strain within a bone cross section subjected to multiaxial loading.[27] Integrating the VA-BATTS tool with internal 3-dimensional bone forces derived from musculoskeletal modeling affords us the ability to efficiently estimate participant-specific bone stress across the load cycle.[14] This integrative approach is useful for larger scale studies seeking to quantify bone loading in specific regions of the tibia under a variety of conditions while providing a basis to make comparisons across participants.

In separate studies, peak tibial stress has been modeled in young adults during walking and running. An examination of tibial loads across studies indicates that running is associated with much greater tibial stress than walking.[30,31,46] However, tibial stresses during walking and running have not been examined in the same study. Additionally, sex differences have not been examined. Because bone loads strongly influence cycles to fatigue and failure, a better understanding of tibial loads in both sexes during walking and running using consistent methodology is needed to design safe progressive exercises.

The purpose of this study was to compare peak and per-step bone stress during walking and 3 speeds of running in female and male recreational runners. We hypothesized that peak loads would be greatest in the fastest running condition. However, stance time shortens as gait speed increases. Thus, we expected slower gait speeds to be associated with greater total per-step loads. Given the disparity in BSI occurrence between men and women, sex differences in tibial stress across conditions were also explored. We hypothesized that women would display greater tibial stress than men.

METHODS

Participants

All participants gave informed written consent to participate in this study, which was approved by the university's institutional human subjects research board. Participants from the local community were recruited by flyers, an email campaign, and website announcements. All volunteers who met the study inclusion and exclusion criteria (n = 40) were enrolled (Table 1), and no participants dropped out. Inclusion criteria included the following: 18 to 35 years of age, presently running more than 16 km/wk, and a treadmill comfort score of $\geq$7 of 10 (completely comfortable). The inclusion criterion of weekly running volume was selected to ensure the safety of participants across treadmill gait speeds during study participation and to enable the generalization of results to the running community and recreational athletes. Exclusion criteria included current musculoskeletal injuries or pain with activity, neuromuscular or cardiopulmonary conditions that could impair normal running function, or contraindications to magnetic resonance imaging (MRI).

Protocol

Upon arrival to the biomechanics laboratory, participants completed a health history and the Bone-specific Physical Activity Questionnaire[55] (intraclass correlation coefficient = 0.92-0.97[54]) for sample characterization because of its positive association with bone density[55] and geometry.[25] Height and weight were obtained, and participants were fitted with standardized laboratory shoes (ProGrid Ride; Saucony) for gait testing. Next, 55 retroreflective markers were placed on participants' bilateral lower extremities and trunk for motion analysis in the manner of Baggaley et al.[2] During all motion capture trials, 3-dimensional marker coordinates and force data were collected with a 10-camera motion analysis system (200 Hz; Qualisys) and an instrumented force treadmill (1000 Hz; Bertec), respectively. A static motion calibration trial and functional hip joint trial were performed to define the lower extremity coordinate systems and joint centers for subsequent motion analysis.[29] Hip joint centers were determined from the trajectories of the thigh markers during active hip rotation using a spherical fit algorithm.[29] The knee and ankle joint centers were calculated as the midpoint of the markers placed on the femoral condyles and malleoli, respectively.

Participants performed an 8-minute, progressive walk-to-run warm-up on the treadmill, during which a self-selected preferred running speed was determined. Preferred running speed was operationally defined as the pace used during a standard, endurance-paced training

*Address correspondence to Stacey A. Meardon, PT, PhD, Department of Physical Therapy, East Carolina University, 2405E Health Sciences Building, Greenville, NC 27834, USA (email: meardons@ecu.edu) (Twitter: @StaceyMeardon).
†Department of Physical Therapy, East Carolina University, Greenville, North Carolina, USA.
‡Department of Kinesiology, Iowa State University, Ames, Iowa, USA.
§Faculty of Kinesiology, University of Calgary, Calgary, Alberta, Canada.
‖Eastern Radiologists, Greenville, North Carolina, USA.
¶School of Physical Therapy and Rehabilitation Science, University of Montana, Missoula, Montana, USA.
Submitted June 19, 2020; accepted January 25, 2021.
One or more of the authors has declared the following potential conflict of interest or source of funding: This work was funded in part by the National Science Foundation's Biomedical Engineering in Simulations, Imaging and Modeling Research Experiences for Undergraduates (award #1359183). AOSSM checks author disclosures against the Open Payments Database (OPD). AOSSM has not conducted an independent investigation on the OPD and disclaims any liability or responsibility relating thereto.

TABLE 1
Participant Demographics and BPAQ Scores[a]

	Female (n = 20)	Male (n = 20)	*P* Value	η_p^2 Value
Age, y	24.65 (23.16-26.14)	24.95 (22.87-27.03)	.81	0.002
Height, cm	167.97 (165.18-171.76)	181.30 (178.44-184.17)	<.001	0.56
Weight, kg	58.22 (53.99-62.45)	80.08 (76.13-84.02)	<.001	0.62
Preferred run speed, m/s	2.79 (2.66-2.92)	2.97 (2.89-3.05)	.02	0.13
Weekly training volume, km	30.98 (23.72-38.24)	24.34 (17.90-30.78)	.16	0.51
Current BPAQ score	6.67 (4.04-9.31)	7.83 (5.59-10.06)	.49	0.01
Previous BPAQ score	50.90 (40.91-60.89)	53.59 (39.15-68.02)	.75	0.003
Total BPAQ score	28.79 (23.44-34.14)	30.73 (23.08-38.38)	.67	0.005

[a]Data are shown as mean (95% CI). The Bone-specific Physical Activity Questionnaire (BPAQ; www.fithdysign.com/BPAQ/) is composed of 2 scores: a previous one and a current one that quantify physical activity more than 1 year before testing and in the past 12 months, respectively. The total BPAQ score is the average of both the previous and current BPAQ scores. Sex differences were examined using *t* tests and partial eta-squared (η_p^2) effect sizes.

run. Next, participants completed 4 gait speed conditions on the treadmill in a randomized order: walking (1.3 m/s), running (preferred running speed), slow running (90% of preferred running speed), and fast running (110% of preferred running speed). Participants were given a 2-minute acclimation period for each gait speed condition before data collection and a minimum of 2 minutes' rest between each condition. Then, 3-dimensional force and marker data were collected for 15 seconds in each condition and processed using real-time motion capture acquisition and processing software (The MotionMonitor; Innovative Sports Training).

Each participant underwent sagittal-, axial-, and coronal-plane MRI of their right tibia using a 1.5-T scanner with a torso coil (Achieva; Philips). All MRI examinations included an axial T1-weighted turbo spin echo (TSE) sequence (TSE factor, 3-4; 7-mm thickness/2-mm gap; field of view, 220; number of excitations, 1; repetition time, 400-600 milliseconds; echo time, 12 milliseconds) as well as coronal and sagittal T1-weighted TSE sequences (TSE factor, 3-4; 4-mm thickness/1-mm gap; field of view, 480; number of excitations, 1; repetition time, 400-600 milliseconds; echo time, 15 milliseconds). Skin markers (vitamin E capsules) mirroring marker placement were placed on the medial and lateral malleoli and proximal right tibia to enable alignment of the MRI tibial coordinate system with motion capture data.

Data Analysis

Axial MRI scans corresponding to the distal one-third cross-section of the tibia, a common site of BSI,[39] were imported into MATLAB (MathWorks) using VA-BATTS bone segmentation subroutines (Figure 1).[26,27] After the rotation of images into the laboratory coordinate system, periosteal and endosteal cortical boundaries were identified using a semiautomatic algorithm, and participant-specific finite element bone meshes were created (10 radial nodes, 60 circumferential nodes). Each mesh was assigned a homogeneous Young modulus of 17.0[44] and a Poisson ratio of 0.3.[45,58] Bone geometry values (cross-sectional area, maximum and minimum second moment of area, and polar moment of inertia) were determined. Additionally, bending and torsional bone strength indices (BSI_B and BSI_T, respectively) were estimated, with I_{max} and J representing the maximum second moment of area and polar moment of inertia, respectively, and l and d representing the tibial length and diameter, respectively[48]:

$$BSI_B = \frac{I_{max}}{ld} \quad (1)$$

and

$$BSI_T = \frac{J}{ld}. \quad (2)$$

Marker trajectory and ground-reaction force data were filtered with a fourth-order, zero-lag low-pass Butterworth filter with a 15-Hz cutoff. With respect to the proximal segments, 3-dimensional Cardan segment and joint angles were calculated in the following order of rotations: flexion/extension, abduction/adduction, and internal/external rotation. Lower extremity joint reaction forces and moments were derived using a rigid body model, estimated body segment parameters,[13] and Newton-Euler inverse dynamics. For the purposes of stance detection, ground-reaction force data were filtered separately with a fourth-order, zero-lag low-pass Butterworth filter with a 50-Hz cutoff. Initial contact and toe-off were defined as the instant that the vertical ground-reaction force exceeded 20 N. For 10 stance phases of each condition, right lower extremity joint angles, reaction forces and moments relative to the proximal coordinate system were exported and input to an integrative musculoskeletal model (Figure 1).[14]

Anthropometrics (height, weight, foot length, shank length, thigh length, and pelvis width) were used to scale the base skeletal model and estimate muscle properties (attachment sites, muscle length, tendon length, cross-sectional area, and pennation angles) for 44 muscles.[1] Trial-specific joint angles were used to create the musculoskeletal models and calculate muscle orientations and moment arms. Using previously estimated force-velocity, passive and active length-tension, and tendon force-extension relationships, maximal forces were estimated for each

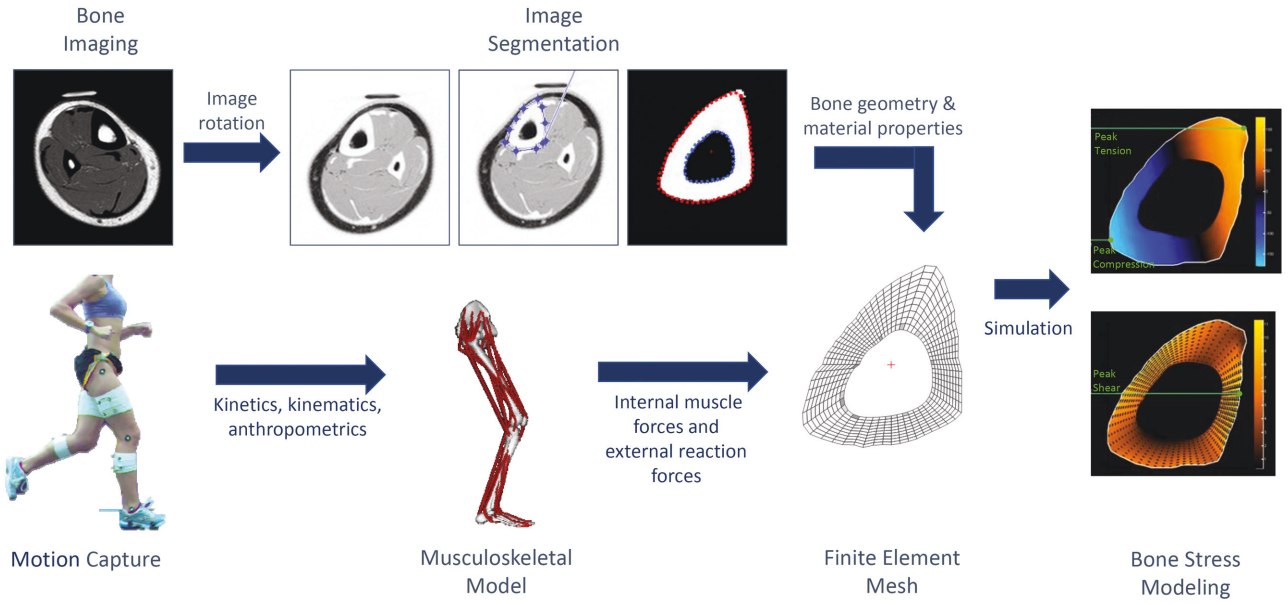

Figure 1. Graphical display of the workflow to estimate bone stress across the stance phase of gait.

muscle at each percentage of stance.[1,12] Maximal muscle force estimations across 101 points of stance served as a boundary condition during muscle force optimization.

Using static optimization, muscle forces at each percentage of stance were estimated with a cost function that minimized the sum of the squared muscle stresses.[22] This cost function allowed for greater load sharing across muscles compared with linear criteria[40] and corresponds well with measured electromyography data during walking and running.[22] Muscle force solutions were constrained such that individual muscle force solutions (1) were bound by zero and the previously derived length- and velocity-adjusted maximal muscle forces as well as (2) matched the joint moments derived from inverse dynamics. A detailed description of the optimization procedure used has been reported by Edwards et al.[15]

Forces acting at the centroid of interest were calculated by translating the ankle joint contact force to the distal one-third part of the tibia. The 3-dimensional ankle joint contact force in the tibial coordinate system was determined by vectorially summing the ankle joint reaction force with estimated muscle forces (medial gastrocnemius, lateral gastrocnemius, soleus, tibialis posterior, flexor digitorum longus, flexor hallucis longus, tibialis anterior, peroneus brevis, peroneus longus, peroneus tertius, extensor digitorum longus, and extensor hallucis longus). Centroid moments were calculated by taking the cross-product of the displacement vector from the centroid to the ankle joint center and the ankle joint contact force. Trial-specific centroid forces and moments were applied to participant-specific cross-sectional finite element meshes. Bending and shear stresses across the stance phase were estimated using beam theory and the finite element method.[26,27]

For each condition and trial, the peak stress values for compression, tension, and shear were collected. Additionally, peak stress at each percentage of the stance phase was obtained to represent compressive, tensile, and shear stress-time curves. The stress-time impulse for each curve was then obtained by calculating the area under each stress curve to represent the total per-step load. Participant data were averaged across trials within each condition and exported for statistical analysis. To aid in data interpretation, bone geometry, bone strength indices, and peak tibial forces and moments were also exported.

Statistical Analysis

After the inspection of data for normality, the potential confounding effect of sex differences on running-related bone stress was examined using repeated-measures analysis of variance, with preferred running speed as a covariate. Then, 2-factor multivariate analyses of variance (MANOVAs) (speed*sex), with speed as a repeated measure, and partial eta-squared (η_p^2) effect sizes[3] were used to evaluate main and interaction effects of speed and sex on both peak stress and stress-time impulse ($\alpha = .05$). When multivariate results were statistically significant, univariate results of component stresses (compression, tension, and shear) were examined. Variances in the differences between all combinations of related groups were assessed using the Mauchly test of sphericity. In instances when sphericity was violated, the Huynh-Feldt correction was utilized. In the absence of an interaction effect, the main effects of sex and speed were examined, and post hoc pairwise comparisons with the Bonferroni adjustment using all participants were performed to examine the effect of speed on measures of stress ($\alpha = .05$). When interactions were observed, the magnitude of change between conditions was compared between sexes post hoc using independent

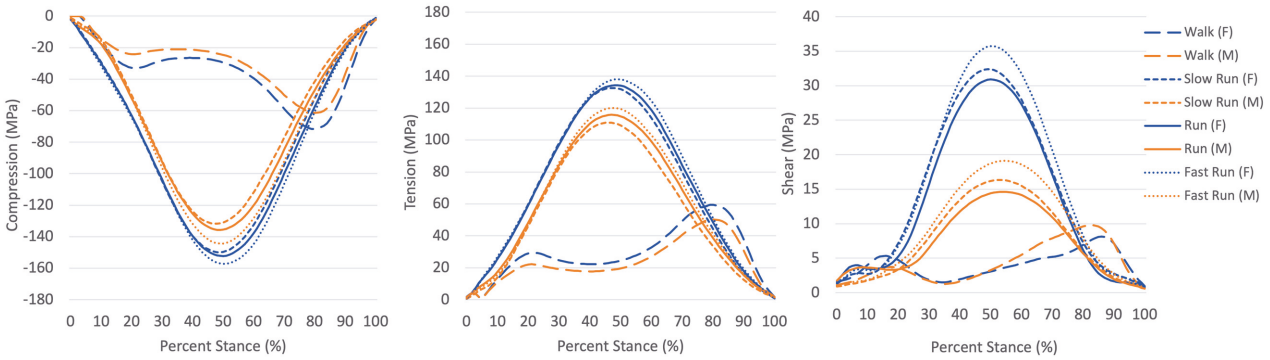

Figure 2. Ensemble time-series curves for both male and female runners during walking, slow running, running, and fast running.

t tests ($\alpha = .05$). If ordinal interactions were observed, the main effect of sex was examined. Potential explanatory variables were compared for descriptive purposes. The required sample sizes computed a priori for within- and between-factors repeated-measures MANOVAs using a type I error probability of .05, power of 0.80, and moderate effect size ($\eta_p^2 = 0.13$) were 14 and 36, respectively (G*Power 3.1).[17,19]

RESULTS

Demographics

Female and male runners differed in height, weight, and preferred running speed (Table 1). An examination of sex differences across running speeds revealed that preferred running speed was not a significant covariate for peak stress or stress-time impulse ($P = .13$-$.96$; $\eta_p^2 = 0.001$-0.06); preferred running speed as a covariate was removed from further analysis.

Peak Bone Stress

Time-series curves indicated that peak stress in both women and men occurred in the midstance during running and in the late stance during walking (Figure 2). The mixed-model within-participant MANOVA revealed a speed*sex interaction for peak stress ($P < .001$; Wilks $\Lambda = 0.59$; $\eta_p^2 = 0.16$). The between-participant MANOVA also indicated sex differences in peak stress values ($P < .001$; Wilks $\Lambda = 0.59$; $\eta_p^2 = 0.41$).

For peak compression, univariate results revealed the main effects of speed ($P < .001$; $\eta_p^2 = 0.95$) and sex ($P = .02$; $\eta_p^2 = 0.13$), with women displaying greater compression than men (Figure 3). Compressive stress was greater at all run speeds compared with walking as well as at the fast speed compared with the slow and preferred speeds (Figure 3). Ordinal speed*sex interactions were observed for peak tension ($P = .001$; $\eta_p^2 = 0.15$) and shear ($P < .001$; $\eta_p^2 = 0.36$) (Figure 3). Women displayed greater peak tension ($P = .001$; $\eta_p^2 = 0.27$) and shear ($P = .001$; $\eta_p^2 = 0.26$) than did men. Mean difference plots and post hoc comparisons of the between-condition magnitude of change (Figure 4) revealed that women, compared with men, demonstrated a greater increase in peak tension ($P = .001$; $\eta_p^2 = 0.23$) and shear ($P < .001$; $\eta_p^2 = 0.38$) when transitioning from a walk to a run. Changes in peak tension and shear between running speeds were similar for both sexes ($P = .14$-$.53$ and $P = .65$-$.85$, respectively). Like compression, tension and shear stress were greater at all run speeds compared with walking (Figure 3). The effect of running speed on tension differed by sex, and like compression, shear stress was greater in the fast running condition compared with the slow and preferred conditions for both sexes (Figure 3).

Stress-Time Impulse

The mixed-model within-participant MANOVA revealed a speed*sex interaction ($P = .03$; Wilks $\Lambda = 0.57$; $\eta_p^2 = 0.43$) for stress-time impulse. Like peak stress, between-participant sex effects were observed for stress-time impulse ($P < .001$; Wilks $\Lambda = 0.58$; $\eta_p^2 = 0.42$).

Univariate results of compressive and tensile stress-time impulse revealed significant main effects of speed ($P < .001$, $\eta_p^2 = 0.50$; and $P = .002$, $\eta_p^2 = 0.14$, respectively) and sex ($P = .006$, $\eta_p^2 = 0.18$; and $P = .001$, $\eta_p^2 = 0.27$, respectively), with women displaying greater impulse than men. Compressive impulse was greater during walking compared with running, whereas tensile impulse was greater during walking and slow running than during fast running (Figure 5). An ordinal speed*sex interaction was observed for shear stress-time impulse ($P < .001$; $\eta_p^2 = 0.23$), with women displaying greater impulse than men ($P < .001$; $\eta_p^2 = 0.33$). A post hoc comparison of the magnitude of change between speeds revealed that women experienced a greater increase in shear stress-time impulse when transitioning from a walk to a slow run than did men ($P < .001$; $\eta_p^2 = 0.29$). Between running speeds, both sexes experienced similar changes in shear stress-time impulse ($P = .23$-$.99$). Post hoc comparisons of speed conditions confirmed that women displayed lower shear impulse during walking compared with slow

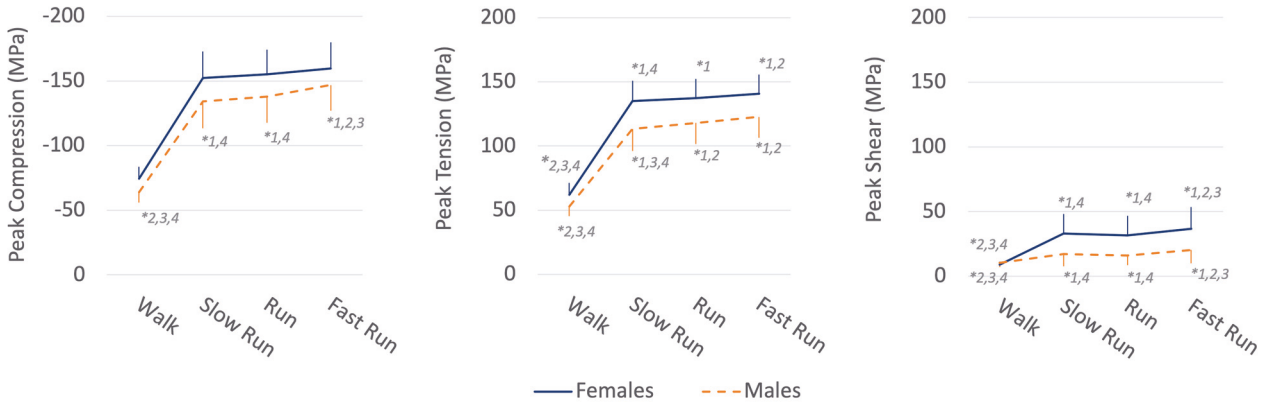

Figure 3. Univariate peak results (mean and 95% CI) across gait speeds are displayed, with post hoc statistically significant ($P < .05$) comparisons noted with asterisks (*) and numerical comparators (1: walk; 2: slow run; 3: preferred run; 4: fast run). Ordinal speed*sex interactions for tension and shear were observed; post hoc comparisons for men and women are displayed separately. Examining the slopes of the change between speeds, women appeared to demonstrate a greater increase in peak tension and shear than men when transitioning from a walk to a run.

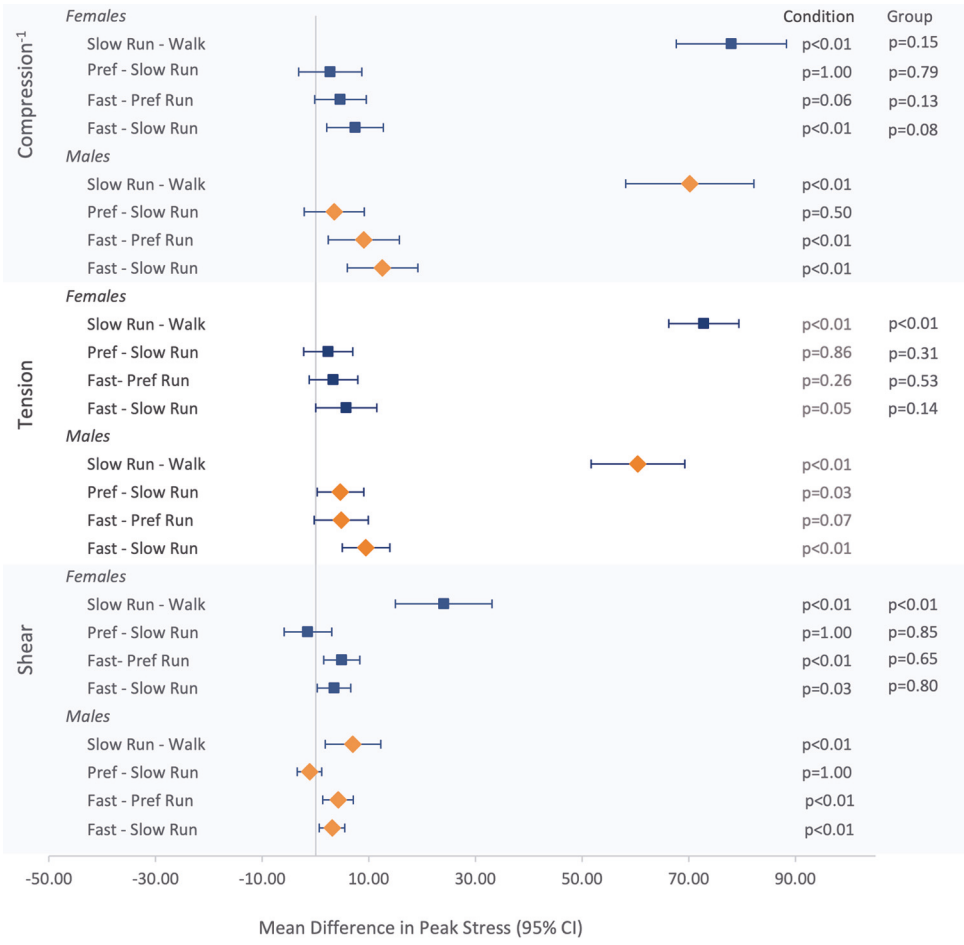

Figure 4. Mean difference plots display sex-specific gait speed differences and 95% CI of the differences. The largest stress differences between speeds were observed when transitioning from a walk to a run for both sexes, with greater stress increases generally observed in women (squares) versus men (diamonds). *P* values for both speed and sex comparisons are listed in the right-hand columns.

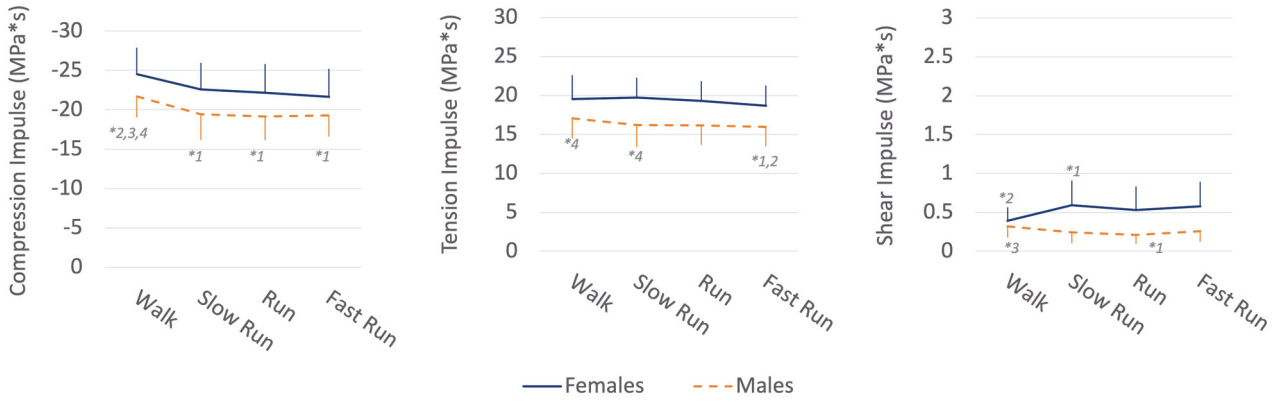

Figure 5. Univariate results for stress-time impulse (mean and 95% CI) across gait speeds are displayed, with post hoc statistically significant ($P < .05$) comparisons noted with asterisks (*) and numerical comparators (1: walk; 2: slow run; 3: preferred run; 4: fast run). An ordinal speed*sex interaction for shear was observed; post hoc comparisons for men and women are displayed separately. Examining the slopes of the change between speeds, women appeared to demonstrate an increase in shear stress-time impulse when transitioning to a run, whereas men experienced a decrease.

TABLE 2
Tibial Structural Characteristics[a]

	Female	Male	*P* Value	η_p^2 Value
Bone geometry				
CSA, mm^2	233.44 (217.17-250.72)	332.75 (316.47-349.03)	<.001	0.67
I_{max}, mm^4	11,420.62 (9475.97-13,366.27)	22,511.19 (20,566.54-24,457.84)	<.001	0.64
I_{min}, mm^4	6136.45 (5159.57-7114.33)	11,225.25 (10,247.37-12,203.12)	<.001	0.59
J, mm^4	17,557.07 (14,852.49-20,262.65)	33,736.44 (31,032.86-36,441.02)	<.001	0.66
Bone strength indices				
BSI_B, mm^2	1.72 (1.48-1.96)	2.59 (2.36-2.83)	<.001	0.43
BSI_T, mm^2	2.65 (2.31-2.98)	3.90 (3.56-4.23)	<.001	0.43

[a]Data are shown as mean (95% CI). Sex differences were examined using *t* tests and partial eta-squared (η_p^2) effect sizes. BSI_B, bending bone strength index; BSI_T, torsional bone strength index; CSA, cross-sectional area; I_{max}, maximum second moment of area; I_{min}, minimum second moment of area; J, polar moment of inertia.

running, while men displayed lower shear impulse during preferred running compared with walking (Figure 5).

Explanatory Variables

Men and women differed in the structural characteristics of bone (Table 2). Women displayed smaller bone geometry values for all measures ($P < .001$; $\eta_p^2 = 0.59$-0.67). Additionally, bone strength indices were lower in women than in men ($P < .001$; $\eta_p^2 = 0.43$).

Component peak tibial forces and moments are displayed in Figure 6. Women displayed lower axial tibial forces across all speeds ($P < .001$; $\eta_p^2 = 0.50$-0.69), lower anterior-posterior forces during walking ($P = .035$; $\eta_p^2 = 0.112$), and greater medial-lateral forces during running ($P \leq .001$; $\eta_p^2 = 0.27$-0.29). Women also displayed lower torsional and medial-lateral bending moments during walking ($P \leq .001$; $\eta_p^2 = 0.36$-0.56) and lower anterior-posterior bending moments across all speeds ($P < .001$; $\eta_p^2 = 0.51$-0.63).

DISCUSSION

The primary purpose of this study was to compare peak and per-step tibial stress during walking and running in both men and women. Secondarily, sex differences in tibial stress metrics were explored. For both sexes, peak stresses markedly increased when transitioning from walking to running, generally increased with faster running speeds, and were highest at the fast running speed, as hypothesized. Contrary to our hypothesis, per-step measures did not uniformly decrease with increasing gait speed; rather, results differed across stress components and sex. Compressive stress-time impulse decreased when transitioning from a walk to a run but did not differ between running speeds. Tensile stress-time impulse was less at the fast run speed compared with walking and slow running, but there was no difference between fast and preferred running. Shear stress-time impulse was sex dependent.

Bone stress during walking and running has been examined in young adults in separate studies, but bone stress across a spectrum of gait speeds has not been

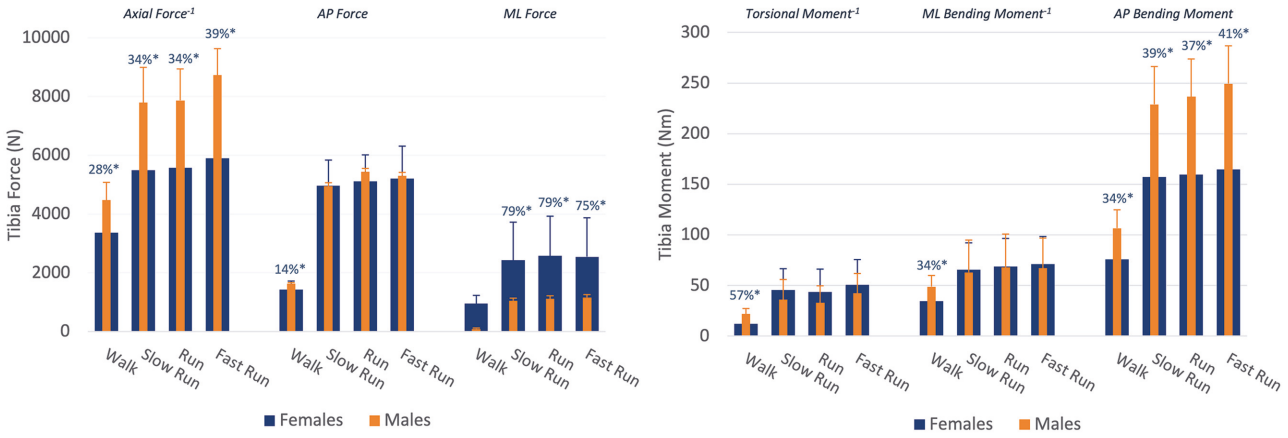

Figure 6. A speed*sex comparison of peak internal tibial forces and moments acting at the distal one-third part of the tibia during stance is displayed (mean and 95% CI). For descriptive purposes, percentage differences in statistically significant comparisons (indicated by *) are reported. Positive force values indicate tension as well as anterior and lateral shear. Positive moment values indicate internal torsion, medial tibial compression, and posterior tibial compression. For display purposes, the axial force and torsional moment are exponentially reported (–1) and thus are negative values. AP, anterior-posterior; ML, mediolateral.

assessed.[30,31,46] Comparing walking with running, we observed marked increases in tibial forces and moments, translating to a greater than 2-fold increase in bone stress. We also found that bone stress increased with faster running speeds; 10% to 20% increases in running speed resulted in 2% to 9% increased compression and tension and 10% to 26% increased shear stress. These results are consistent with those of Yang et al[59] and Edwards et al,[16] who found that 25% to 33% faster running speeds corresponded to 8% to 16% greater bone strain and a 7% to 10% greater probability of failure. In combination with these previous studies, our results have direct clinical implications for athlete and physical activity preparedness. First, the marked tibial stress increase during running compared with walking suggests that transitional activities may be needed when preparing athletes for running-related stresses to gradually expose bone to higher magnitude loads to ensure positive bone adaptation and minimize the injury risk. Second, in the at-risk athlete, the increase in bone stress across running speeds is not trivial; small increases in bone loads result in an exponential decrease in the number of bone loading cycles to failure,[8] suggesting that rapid increases in running speed should be avoided.

Animal models of fatigue loading suggest that the magnitude of loading, rate of loading, and number of load cycles influence bone turnover and the injury risk.[50] Load impulse (area under the waveform curve) captures the magnitude, rate, and temporal features of loading and may be a useful per-step metric to monitor load exposure or cumulative load. In recent years, cumulative measures of loading have been identified as important to understand both acute and chronic workloads associated with an injury,[10,52] and per-step load metrics have been linked with musculoskeletal injuries.[4,11] To date, per-step tibial stress has not been reported for running or compared across a range of gait speeds. Compared with previous measures of cumulative tibial loading,[23] tibial stress-time impulse, as calculated in this study, provided a comprehensive per-step metric that incorporated 3-dimensional forces and moments as well as participant-specific bone structure. We found that compared with walking, running tended to have a lower stress-time impulse. This is generally consistent with previous studies examining the impulse of lower extremity joint loads during walking and running.[24,36,47] Similar to Petersen et al,[41] we did not observe a significant variance in stress-time impulse across running speeds. The importance of stress-time impulse versus other waveform characteristics in the development of BSIs ex vivo is relatively unknown. On mechanical testing, Nalla et al[38] found that under low stress, cortical bone was more susceptible to cyclic fatigue versus creep mechanisms; at comparatively higher stress, cortical bone displayed both time-dependent ("creep") and cycle-dependent (fatigue) crack propagation at similar rates. These same authors also reported that under low stress, higher frequency loads (10 Hz) resulted in less crack extension than low frequency loads (1 Hz); however, under higher stress, crack extension was comparable for both high and low frequency loading.[38] It is possible that stress-time impulse with respect to injuries may be dependent on stress magnitude, with stress-time impulse more relevant under low stress conditions.

Sex differences in running biomechanics and injury occurrence are well-established in the literature.[9,20,56,57] However, sex-related differences in bone stress during walking and running have not been reported. We found that women generally demonstrated greater peak tibial stress and stress-time impulse across all gait speeds and displayed a greater increase in tibial stress magnitude

when transitioning from a walk to a run. These sex differences in bone stress appear to be the result of differences in bone geometry and tibial forces that were not proportionately lower in women, given their smaller stature and lower mass compared with men. Bone geometry between sexes differed by 35% to 65%, with women displaying smaller bone geometry. Yet, an evaluation of sex differences in non–body weight normalized tibial forces revealed that women only displayed lower axial forces (33%-48%) and anterior-posterior bending moments (15%). Anterior-posterior forces, medial-lateral bending moments, and torsional moments were comparable between sexes, and medial-lateral forces were greater in women than in men (54%-57%). The importance of bone characteristics relative to applied loads is supported by Popp et al,[43] who reported that bone strength relative to vertical ground-reaction forces discriminated female runners with BSIs from those without BSIs. Interestingly, despite having comparable bone loading histories, as evidenced by similar bone loading history scores, female runners in this study appeared to display lower bone strength relative to the tibial loads encountered. These sex-related differences may, in part, explain the higher incidence of BSIs in women[56] and suggest that women may need slower acclimation when initiating a running program to allow for bone adaptation.

Sex-related differences in gait mechanics likely underlie the disparity in tibial loads. Women have consistently shown greater frontal and transverse lower extremity joint kinematics across a variety of studies.[9,20,57] In agreement with these studies, our post hoc evaluation of frontal- and transverse-plane biomechanics revealed that women displayed greater hip adduction, knee internal rotation, and peak rearfoot eversion; a narrower step width; and a tendency for a greater medial-lateral ground-reaction force and free moment. These sex differences in gait biomechanics likely contributed to the disparity in medial-lateral loads and the relative disparity in torsional loads between men and women in our study, especially when changing from a walk to a run. Relatedly, frontal and transverse gait mechanics have been linked with tibial BSIs[42] and greater tibial loads.[30,59]

The strengths of this study include the examination of participant-specific walking and running tibial stresses in the same study, direct implications for athletic and physical activity preparedness, examination of sex-related differences, and use of a mixed-sex cohort of recreational runners, which increase generalizability to the running population. However, it is important to note that only acute load estimates were obtained. Bone stress changes with exertion and, given the dynamic nature of bone adaptation, over time. Future work should examine cumulative loads with exposure as well as damage formation indices. Additionally, the results of this study are most generalizable to younger recreational runners. Because of the growing popularity of running across the life span, future studies should aim to build on these results by testing other age groups. Last, musculoskeletal modeling is not without limitations; assumptions were made relative to the anthropometric model, muscle parameters, and optimization criteria, all of which may differ between sexes. We attempted to minimize errors associated with these assumptions by scaling the base skeletal and muscle model to participant-specific anthropometrics, constraining muscle force solutions to match participant- and task-specific joint moments, and using participant-specific bone models in bone stress estimation. Our walking-related stresses were higher than those reported by Derrick et al,[14] most likely because of model input, sex, and condition (treadmill vs overground) differences. However, similar to previous work, modeled tibial stress was affected by loading conditions and group differences,[14,30,31,46] and peak compressive stress occurred posteriorly and tension anteriorly.[30,31,46,59] Additionally, bone stress along the medial border of our tibiae, when converted to strain, fell within the range of previous reports on distal medial tibial strains during human activities (Appendix Figure A1, available in the online version of this article).[6,21,28,32-35]

CONCLUSION

Tibial stress increased more than 2-fold when transitioning from a walk to a run, and varying the running speed by 10% to 20% from a preferred pace elicited proportional changes in bending and shear stress. When compared with men, women displayed greater tibial stress and markedly greater tension and shear stress when transitioning from walking to running. A smaller bone size in women relative to applied loads contributed to elevated tibial stress and may partly explain the sex bias in tibial BSIs. Interventions to reduce injurious bone stress should consider regulating loads encountered during training, especially when transitioning from a walk to a run, and increasing bone strength through targeted exercise programs. Additionally, female runners may need a slower progression when initiating a running program.

ACKNOWLEDGMENT

The authors thank L. Stubbs, Z. Blank, E. Brown, K. Bartol, and L. Goel, who helped with data collection and processing, as well as Dr Ali Vahdati, who assisted in interpretation.

REFERENCES

1. Arnold EM, Ward SR, Lieber RL, Delp SL. A model of the lower limb for analysis of human movement. *Ann Biomed Eng*. 2010;38(2):269-279.
2. Baggaley M, Willy RW, Meardon SA. Primary and secondary effects of real-time feedback to reduce vertical loading rate during running. *Scand J Med Sci Sports*. 2017;27(5):501-507.
3. Bakeman R. Recommended effect size statistics for repeated measures designs. *Behav Res Methods*. 2005;37(3):379-384.
4. Bennell KL, Bowles KA, Wang Y, Cicuttini F, Davies-Tuck M, Hinman RS. Higher dynamic medial knee load predicts greater cartilage loss over 12 months in medial knee osteoarthritis. *Ann Rheum Dis*. 2011;70(10):1770-1774.
5. Burr DB. Bone, exercise, and stress fractures. *Exerc Sport Sci Rev*. 1997;25:171-194.

6. Burr DB, Milgrom C, Fyhrie D, et al. In vivo measurement of human tibial strains during vigorous activity. *Bone*. 1996;18(5):405-410.
7. Burr DB, Radin EL. Microfractures and microcracks in subchondral bone: are they relevant to osteoarthrosis? *Rheum Dis Clin North Am*. 2003;29(4):675-685.
8. Carter DR, Caler WE. A cumulative damage model for bone fracture. *J Orthop Res*. 1985;3(1):84-90.
9. Chumanov ES, Wall-Scheffler C, Heiderscheit BC. Gender differences in walking and running on level and inclined surfaces. *Clin Biomech*. 2008;23(10):1260-1268.
10. Coenen P, Kingma I, Boot CRL, Twisk JWR, Bongers PM, Van Dieën JH. Cumulative low back load at work as a risk factor of low back pain: a prospective cohort study. *J Occup Rehabil*. 2013;23(1):11-18.
11. Colby MJ, Dawson B, Heasman J, Rogalski B, Gabbett TJ. Accelerometer and GPS-derived running loads and injury risk in elite Australian footballers. *J Strength Cond Res*. 2014;28(8):2244-2252.
12. Delp SL, Loan JP, Hoy MG, Zajac FE, Topp EL, Rosen JM. An interactive graphics-based model of the lower extremity to study orthopaedic surgical procedures. *IEEE Trans Biomed Eng*. 1990; 37(8):757-767.
13. Dempster WT, Gabel WC, Felts WJL. The anthropometry of the manual work space for the seated subject. *Am J Phys Anthropol*. 1959;17(4):289-317.
14. Derrick TR, Edwards WB, Fellin RE, Seay JF. An integrative modeling approach for the efficient estimation of cross sectional tibial stresses during locomotion. *J Biomech*. 2016;49(3):429-435.
15. Edwards WB, Gillette JC, Thomas JM, Derrick TR. Internal femoral forces and moments during running: implications for stress fracture development. *Clin Biomech (Bristol, Avon)*. 2008;23(10): 1269-1278.
16. Edwards WB, Taylor D, Rudolphi TJ, Gillette JC, Derrick TR. Effects of running speed on a probabilistic stress fracture model. *Clin Biomech*. 2010;25(4):372-377.
17. Erdfelder E, Faul F, Buchner A, Lang AG. Statistical power analyses using G*Power 3.1: tests for correlation and regression analyses. *Behav Res Methods*. 2009;41(4):1149-1160.
18. Farr JN, Lee VR, Blew RM, Lohman TG, Going SB. Quantifying bone-relevant activity and its relation to bone strength in girls. *Med Sci Sports Exerc*. 2011;43(3):476-483.
19. Faul F, Erdfelder E, Lang AG, Buchner A. G*Power 3: a flexible statistical power analysis program for the social, behavioral, and biomedical sciences. *Behav Res Methods*. 2007;39(2):175-191.
20. Ferber R, Davis IMC, Williams DS. Gender differences in lower extremity mechanics during running. *Clin Biomech*. 2003;18(4):350-357.
21. Fyhrie DP, Milgrom C, Hoshaw SJ, et al. Effect of fatiguing exercise on longitudinal bone strain as related to stress fracture in humans. *Ann Biomed Eng*. 1998;26(4):660-665.
22. Glitsch U, Baumann W. The three-dimensional determination of internal loads in the lower extremity. *J Biomech*. 1997;30(11-12):1123-1131.
23. Hunter JG, Garcia GL, Shim JK, Miller RH. Fast running does not contribute more to cumulative load than slow running. *Med Sci Sports Exerc*. 2019;51(6):1178-1185.
24. Jin L, Hahn ME. Comparison of lower extremity joint mechanics between healthy active young and middle age people in walking and running gait. *Sci Rep*. 2019;9(1):1-8.
25. Kim S, Baker BS, Sharma-Ghimire P, Bemben DA, Bemben MG. Association between bone-specific physical activity scores and pQCT-derived measures of bone strength and geometry in healthy young and middle-aged premenopausal women. *Arch Osteoporos*. 2018;13(1):83.
26. Kourtis L, Kesari H, Carter D, Beaupré G. Transverse and torsional shear stresses in prismatic bodies having inhomogeneous material properties using a new 2D stress function. *J Mech Mater Struct*. 2009;4(4):659-674.
27. Kourtis LC, Carter DR, Kesari H, Beaupre GS. A new software tool (VA-BATTS) to calculate bending, axial, torsional and transverse shear stresses within bone cross sections having inhomogeneous material properties. *Comput Methods Biomech Biomed Engin*. 2008;11(5):463-476.
28. Lanyon LE. Osteocytes, strain detection, bone modeling and remodeling. *Calcif Tissue Int*. 1993;53(suppl 1):S102-S107.
29. Leardini A, Cappozzo A, Catani F, et al. Validation of a functional method for the estimation of hip joint centre location. *J Biomech*. 1999;32(1):99-103.
30. Meardon SA, Derrick TR. Effect of step width manipulation on tibial stress during running. *J Biomech*. 2014;47(11):2738-2744.
31. Meardon SA, Willson JD, Gries SR, Kernozek TW, Derrick TR. Bone stress in runners with tibial stress fracture. *Clin Biomech*. 2015; 30(9):895-902.
32. Milgrom C, Finestone A, Levi Y, et al. Do high impact exercises produce higher tibial strains than running? *Br J Sports Med*. 2000; 34(3):195-199.
33. Milgrom C, Finestone A, Simkin A, et al. In vivo strain measurements to evaluate the strengthening potential of exercises on the tibial bone. *J Bone Joint Surg Br*. 2000;82(4):591-594.
34. Milgrom C, Miligram M, Simkin A, Burr D, Ekenman I, Finestone A. A home exercise program for tibial bone strengthening based on in vivo strain measurements. *Am J Phys Med Rehabil*. 2001;80(6):433-438.
35. Milgrom C, Radeva-Petrova DR, Finestone A, et al. The effect of muscle fatigue on in vivo tibial strains. *J Biomech*. 2007;40(4):845-850.
36. Miller RH, Edwards WB, Brandon SCE, Morton AM, Deluzio KJ. Why don't most runners get knee osteoarthritis? A case for per-unit-distance loads. *Med Sci Sports Exerc*. 2014;46(3):572-579.
37. Nalla RK, Kinney JH, Ritchie RO. Mechanistic fracture criteria for the failure of human cortical bone. *Nat Mater*. 2003;2(3):164-168.
38. Nalla RK, Kruzic JJ, Kinney JH, Ritchie RO. Aspects of in vitro fatigue in human cortical bone: time and cycle dependent crack growth. *Biomaterials*. 2005;26(14):2183-2195.
39. Nattiv A, Kennedy G, Barrack MT, et al. Correlation of MRI grading of bone stress injuries with clinical risk factors and return to play: a 5-year prospective study in collegiate track and field athletes. *Am J Sports Med*. 2013;41(8):1930-1941.
40. Pedersen DR, Brand RA, Cheng C, Arora JS. Direct comparison of muscle force predictions using linear and nonlinear programming. *J Biomech Eng*. 1987;109(3):192-199.
41. Petersen J, Sørensen H, Nielsen RØ. Cumulative loads increase at the knee joint with slow-speed running compared to faster running: a biomechanical study. *J Orthop Sports Phys Ther*. 2015;45(4):316-322.
42. Pohl MB, Mullineaux DR, Milner CE, Hamill J, Davis IS. Biomechanical predictors of retrospective tibial stress fractures in runners. *J Biomech*. 2008;41(6):1160-1165.
43. Popp KL, McDermott W, Hughes JM, Baxter SA, Stovitz SD, Petit MA. Bone strength estimates relative to vertical ground reaction force discriminates women runners with stress fracture history. *Bone*. 2017;94:22-28.
44. Reilly DT, Burstein AH. The elastic and ultimate properties of compact bone tissue. *J Biomech*. 1975;8(6):393-405.
45. Rho JY, Hobatho MC, Ashman RB. Relations of mechanical properties to density and CT numbers in human bone. *Med Eng Phys*. 1995;17(5):347-355.
46. Rice H, Weir G, Trudeau MB, Meardon S, Derrick T, Hamill J. Estimating tibial stress throughout the duration of a treadmill run. *Med Sci Sports Exerc*. 2019;51(11):2257-2264.
47. Schache AG, Lin YC, Crossley KM, Pandy MG. Is running better than walking for reducing hip joint loads? *Med Sci Sports Exerc*. 2018;50(11):2301-2310.
48. Selker F, Carter DR. Scaling of long bone fracture strength with animal mass. *J Biomech*. 1989;22(11-12):1175-1183.
49. Tenforde AS, Sayres LC, McCurdy ML, Sainani KL, Fredericson M. Identifying sex-specific risk factors for stress fractures in adolescent runners. *Med Sci Sports Exerc*. 2013;45(10):1843-1851.
50. Turner CH. Three rules for bone adaptation to mechanical stimuli. *Bone*. 1998;23(5):399-407.
51. Vahdati A, Walscharts S, Jonkers I, Garcia-Aznar JM, Vander Sloten J, van Lenthe GH. Role of subject-specific musculoskeletal loading on the prediction of bone density distribution in the proximal femur. *J Mech Behav Biomed Mater*. 2014;30:244-252.

52. Village J, Frazer M, Cohen M, Leyland A, Park I, Yassi A. Electromyography as a measure of peak and cumulative workload in intermediate care and its relationship to musculoskeletal injury: an exploratory ergonomic study. *Appl Ergon*. 2005;36(5):609-618.
53. Warden SJ, Davis IS, Fredericson M. Management and prevention of bone stress injuries in long-distance runners. *J Orthop Sports Phys Ther*. 2014;44(10):749-765.
54. Weeks B, Hirsch R, Moran D, Beck B. A useful tool for analysing the effects of bone-specific physical activity. *Salud i Cienc*. 2011; 18(6):538-542.
55. Weeks BK, Beck BR. The BPAQ: a bone-specific physical activity assessment instrument. *Osteoporos Int*. 2008;19(11): 1567-1577.
56. Wentz L, Liu PY, Haymes E, Ilich JZ. Females have a greater incidence of stress fractures than males in both military and athletic populations: a systemic review. *Mil Med*. 2011;176(4):420-430.
57. Willson JD, Petrowitz I, Butler RJ, Kernozek TW. Male and female gluteal muscle activity and lower extremity kinematics during running. *Clin Biomech*. 2012;27(10):1052-1057.
58. Wirtz DC, Schiffers N, Forst R, Pandorf T, Weichert D, Radermacher K. Critical evaluation of known bone material properties to realize anisotropic FE-simulation of the proximal femur. *J Biomech*. 2000;33(10):1325-1330.
59. Yang PF, Sanno M, Ganse B, et al. Torsion and antero-posterior bending in the in vivo human tibia loading regimes during walking and running. *PLoS One*. 2014;9(4):e94525.